

PREPARED FOR SUBMISSION TO JINST

TOPICAL WORKSHOP ON ELECTRONICS FOR PARTICLE PHYSICS  
SEPTEMBER 30 – OCTOBER 4 2024  
GLASGOW, SCOTLAND

# Characterization of pre-production petals for the ATLAS Inner Tracker strip detector

---

**M.J. Basso,<sup>a,b,1</sup> on behalf of the ATLAS ITk collaboration**

<sup>a</sup>*TRIUMF, Wesbrook Mall, Vancouver, Canada*

<sup>b</sup>*Department of Physics, Simon Fraser University, University Drive W, Burnaby, Canada*

*E-mail:* [mbasso@triumf.ca](mailto:mbasso@triumf.ca)

**ABSTRACT:** For the High-Luminosity Large Hadron Collider, the ATLAS experiment will replace its current Inner Detector with an all-silicon Inner Tracker (ITk), consisting of pixel and strip systems. In the end-cap, silicon sensor modules of the strip system are mounted onto support structures called “petals”. To facilitate the assembly of petals, an automated system has been developed which streamlines the production process and ensures uniformity. This paper presents the latest results from the assembly of the first ITk pre-production petals, including characterization of their electrical performance and studies of their robustness at temperatures  $\leq -35^\circ\text{C}$ .

**KEYWORDS:** Si microstrip and pad detectors; Detector design and construction technologies and materials; Overall mechanics design

---

<sup>1</sup>Corresponding author.

© 2024 CERN for the benefit of the ATLAS collaboration (CC-BY-4.0 license).



## 1 Introduction

The High-Luminosity (HL) upgrade [1] of the Large Hadron Collider (LHC) [2] will deliver  $3000 \text{ fb}^{-1}$  of data over its lifetime and enable precision measurements of fundamental physics [3, 4]. However, with an order-of-magnitude more collisions per bunch crossing relative to the LHC, the HL-LHC collision environment is also more complex. To accommodate this increased complexity, the ATLAS experiment [5] will replace its existing Inner Detector (ID) [6, 7] with the all-silicon Inner Tracker (ITk) [8]. Relative to the ID, the ITk will feature an improved radiation hardness, higher granularity ( $5 \times 10^9$  channels), enhanced forward coverage ( $|\eta| < 4.0$ ), and a faster response.

The ITk consists of a pixel detector [9] surrounded by a strip detector [10], with the strip detector consisting of four barrel layers and twelve endcap disks, six on each side. Each endcap is composed of 32 double-sided support structures known as “petals” [11], and each side of a petal is composed of nine silicon strip sensors [12]. The nine sensors are grouped into six modules [13, 14] — the fundamental readout units of the strip detector — of different types, labelled R0–R5 in order of increasing radius. Each module consists of PCB flex circuits providing readout and power which are glued and wire-bonded to a sensor. A fully-assembled petal is shown in figure 1.

The remainder of this paper describes how petals are assembled for the production of the ITk as well as how the quality of petals is characterized (section 2). It also describes the reliability of petals at temperatures  $\leq -35^\circ\text{C}$  and the issue of “sensor cracking” (section 3).

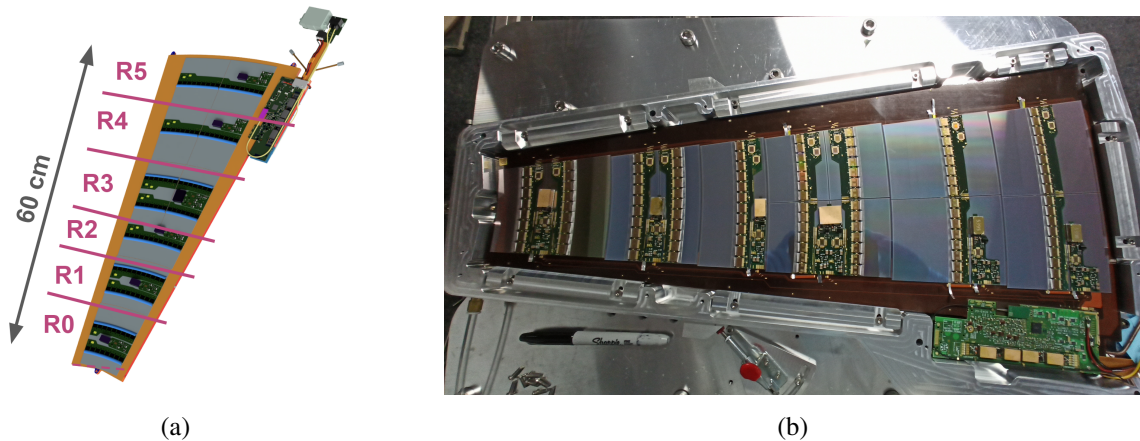


**Figure 1:** (a) A schematic of petal with the different module types (R0–R5) delineated and (b) a picture of a loaded petal.

## 2 Production of petals

A carbon-fibre “core” comprises the support structure of a petal, whose interior is made of a thermally-conductive foam and carbon-fibre honeycomb. Titanium pipes embedded within the foam provide cooling and enable operational temperatures as cold as  $-35^\circ\text{C}$ . On the surface, copper-on-polyimide “bus tapes” route data and power and interface with back-end electronics [15]. Mounting modules onto cores or “loading” occurs at several international sites in Canada, Germany, and Spain. For simplicity and uniformity of production, an automated loading system has been

developed [16, 17], shown in figure 2. The automated system consists of a programmable gantry robot capable of dispensing adhesive as well as lifting and placing modules with micron-level precision using custom vacuum tools. The modules are subsequently wire-bonded to the bus tape. Careful optimization of the choice of adhesive, its deposition pattern, and its dispensed volume has been performed to ensure sufficient coverage of each module’s footprint while minimizing seepage.

An optical alignment system assists in module placement and performs the post-loading placement accuracy survey: by measuring the positions of ten fiducial markers on each sensor, the centre and angle of each module may be determined. Detector alignment and electrical isolation of neighbouring modules requires a placement accuracy of  $50\ \mu\text{m}$ ; however, an accuracy of better than  $20\ \mu\text{m}$  is often achieved, as shown in figure 3a. Post-loading metrology is performed using a confocal displacement sensor or similar, an example of which is shown in figure 3b. Measurements of metrology verify that the modules are mounted flat with an acceptable bow, both of which are requirements for insertion into an endcap. Nearly<sup>2</sup> all pre-production petals assembled thus far have met these mechanical specifications, demonstrating the excellent reliability of the automated loading system.

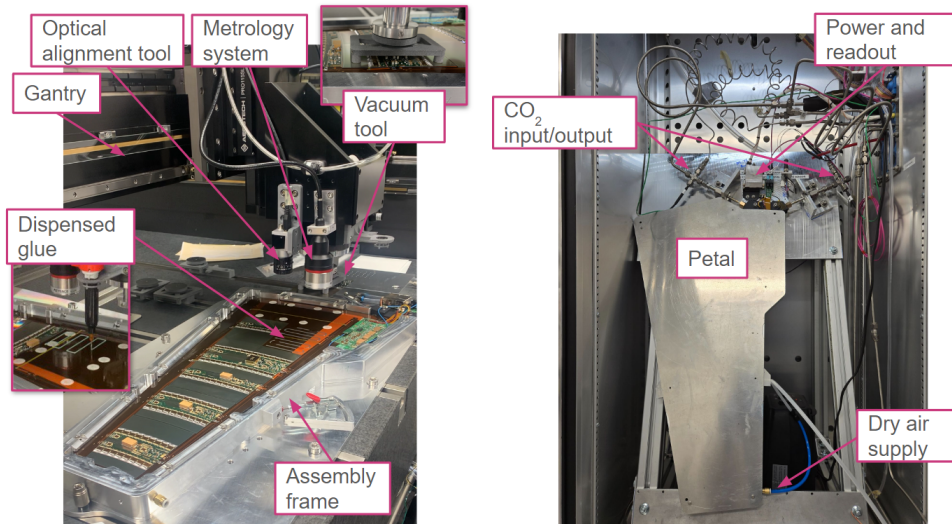


**Figure 2:** Labelled pictures of (left) a petal being actively loaded, with insets showing the dispensed glue and module placement, and (right) a petal in a freezer for electrical testing.

The production quality of loaded petals is further characterized through measurements of their electrical performance. The current-voltage (IV) characteristics of each sensor should satisfy  $< 10\ \mu\text{A}$  at  $500\ \text{V}$  bias to ensure high-voltage (HV) supplies will be able to adequately power the ITk over its lifetime. The per-channel input noise should be low enough at  $350\ \text{V}$  bias to ensure the signal-to-noise ratio of hits is high enough at the ITk’s end-of-life, typically  $< 1000$  units of equivalent noise charge (ENC). Additionally, loading should not significantly alter a module’s IV characteristics or its input noise. To perform these tests, petals are mounted in a light-tight freezer under controlled temperature and humidity, shown in figure 2. To maintain a constant temperature, liquid  $\text{CO}_2$  or ethanol is flowed through the core’s cooling pipes, the former relying on a MARTA

<sup>2</sup>Nearly, as a few pre-production petals have been out-of-specification but for known reasons.

cooling plant [18]. Measurements of both the IV characteristics and input noise are performed using the ITk’s data acquisition (DAQ) software [13, 19]. An example of the input noise for an R3 module before and after loading is shown in figure 3c; to date, all modules have exhibited excellent consistency in their electrical performance before and after loading.

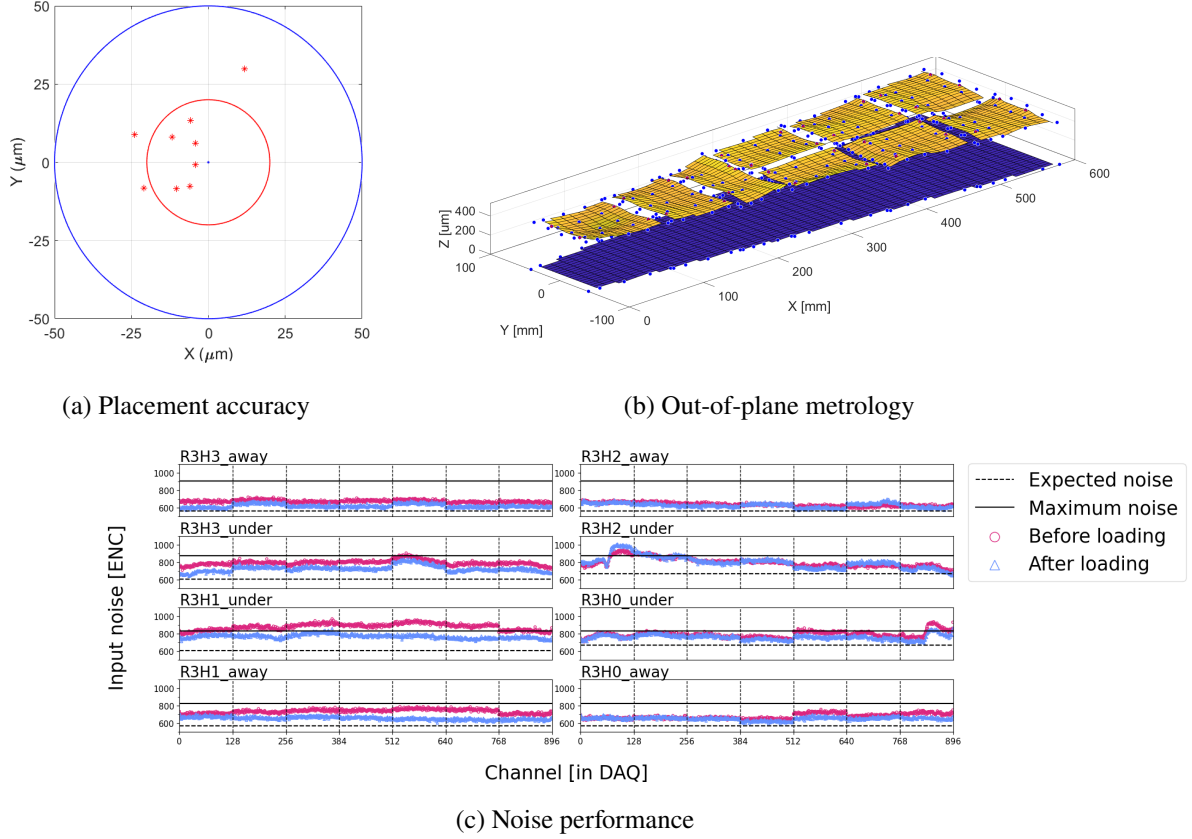


**Figure 3:** Examples of metrics characterizing the production quality of petals. (a) Placement accuracy of modules, indicated by the red stars; the blue circle ( $\pm 50 \mu\text{m}$ ) indicates specification. (b) Out-of-plane metrology, with the modules (orange surfaces) offset from the core (blue surface) by  $\sim 400 \mu\text{m}$ . (c) Input noise performance for an R3 module, before and after loading.

### 3 Reliability testing of petals

It was observed that  $\sim 10\%$  of modules on cores (in the barrel layers or the endcaps) exhibited HV breakdown — an immediate and held increase in current — at biases  $\lesssim 100 \text{ V}$  in the relevant temperature range for quality control,  $-35 \text{ }^\circ\text{C}$  or colder. The HV breakdowns were found to be a result of cracks in the silicon sensors [20, 21], and these cracks were found to occur predominantly in the sensor areas between flexes. This is understood to result from a mismatch in the coefficients of thermal expansion between the copper in the flexes and the silicon sensor: at cold temperatures, the copper contracts more than the silicon, creating localized areas of stress on the sensors. This mechanism has been corroborated by mechanical simulations [22]. Additionally, while IV characteristics indicate the presence of a possible crack, measurements of the per-channel input noise

localize its position, as cracks result in very low or high noise for the channels they intersect. A picture of a crack and the corresponding IV measurements are shown in figure 4.

Understanding and resolving sensor cracking is one of the most urgent issues for the ITK project at the present. To investigate its prevalence, petals have been thermal cycled from  $-35\text{ }^{\circ}\text{C}$  to progressively colder temperatures using a climate chamber or similar. After each cycle, the electrical performance of each petal has been measured to check for the formation of cracks. For the first petal made of production-quality parts, cracks were already observed after the  $-40\text{ }^{\circ}\text{C}$  thermal cycle, and so a campaign was launched to explore potential mitigation strategies.

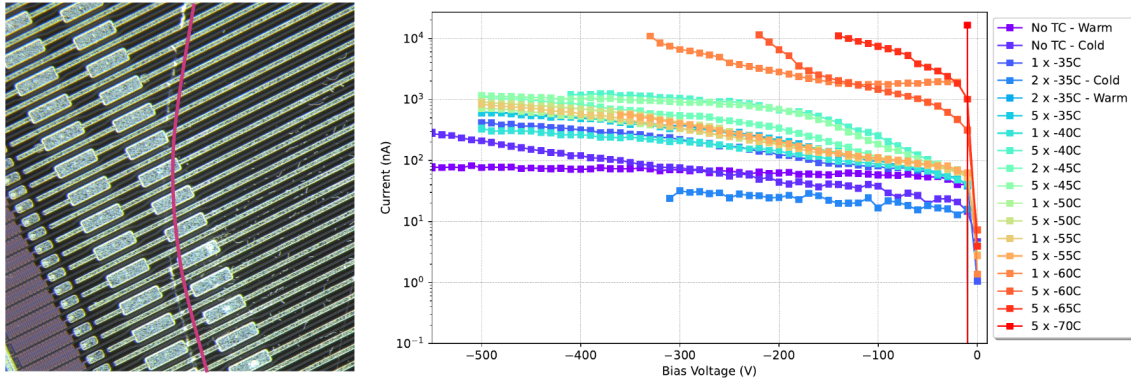


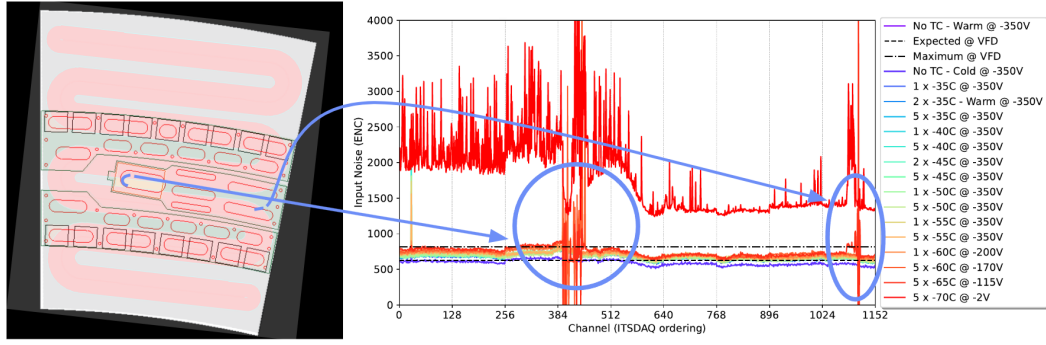
**Figure 4:** (Left) Picture of a crack (left of the red line) on the sensor of an R0 module and (right) the corresponding IV measurements for each thermal cycle (TC). In the legend, “ $N \times Y\text{C}$ ” corresponds to  $N$  thermal cycles at temperature  $Y\text{ }^{\circ}\text{C}$ . HV breakdown is visible after the  $-60\text{ }^{\circ}\text{C}$  thermal cycle.

The importance of the choice of adhesive and its pattern during loading have been confirmed by mechanical simulations. The glue nominally used is Dow SE4445 [23] in a “snake-like” pattern. Simulation identified that using glue with a higher Young’s modulus, such as Loctite EA9396 (“HYSOL”) [24], can reduce stress by 50%, and so a second petal was loaded using HYSOL in the same pattern. However, 20 cracks were observed (out of 23 suspected), the first occurring after the  $-35\text{ }^{\circ}\text{C}$  thermal cycle. A mechanical analysis of SE4445 revealed that its modulus increases from  $\mathcal{O}(0.1)$  MPa for temperatures  $\gtrsim -40\text{ }^{\circ}\text{C}$  to  $\mathcal{O}(100)$  MPa for temperatures  $\lesssim -45\text{ }^{\circ}\text{C}$ , the latter being comparable to that of HYSOL. Simulation informs of the relative change in stress resulting from design choices, explaining why the use of HYSOL did not lead to an improvement on its own.

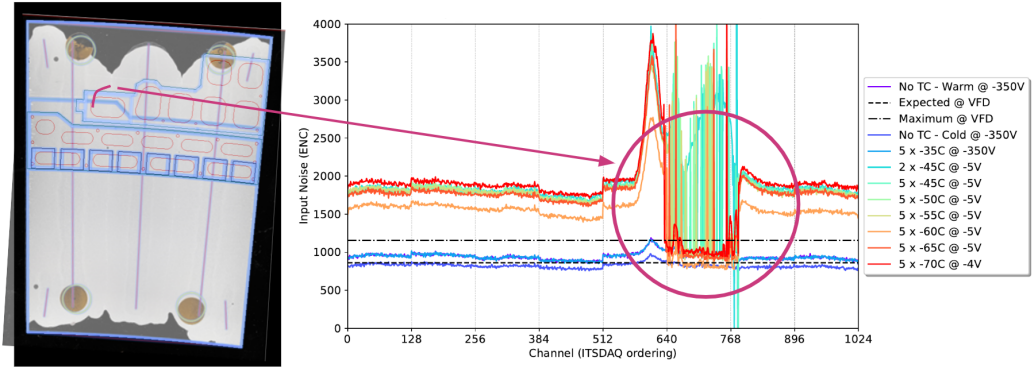
Many of the cracks from the snake-like HYSOL petal occurred along the edges of the glue pattern used for loading, as shown in figure 5a, suggesting that edges are not well supported. A second petal was loaded using HYSOL in a “full-coverage” pattern, which was optimized to cover as much of the core-sensor interface as possible. However, eleven cracks were still observed, and one notably occurred after the  $-45\text{ }^{\circ}\text{C}$  thermal cycle in a region well supported by HYSOL, as shown in figure 5b. Accordingly, this design choice was an improvement but not sufficient.

Other mitigation strategies are being pursued as well. The ten remaining cracks on the full-coverage HYSOL petal all occurred in regions near the “glue dots” used in the module glue pattern, indicated by the small red circles in the glue patterns of figure 5. Simulation has shown the glue dots to result in localized stress, and so a third petal will be built using modules whose glue patterns do not use glue dots. The inclusion of a flexible glue layer or “interposer” within modules can also





(a) R0 module from the snake-like HYSOL petal



(b) R4 module from the full-coverage HYSOL petal

**Figure 5:** (Left) Pictures of the HYSOL patterns used for loading two example modules and (right) the corresponding noise distributions measured after each thermal cycle. Both modules exhibited cracking. On the left side of (a) ((b)), the loading pattern is indicated in light red shading (grey fill) and the observed cracks are indicated by the blue (red) lines. In the legend, “ $N \times YC$ ” corresponds to  $N$  thermal cycles at temperature  $Y^\circ C$ ; the bias voltage for each measurement is also indicated.

reduce stress by 95% and has been shown to be a promising solution for loaded cores in the barrel layers, and so a fourth petal will be built interposer modules. These efforts are ongoing.

#### 4 Conclusion

This paper presented the procedures for building and testing production-quality petals for the ATLAS ITk. By using an automated assembly system, the petals built thus far have met both their mechanical and electrical specifications. This paper also addressed the steps taken to address sensor cracking on petals, a complex and urgent issue. Two mitigation strategies relating to the choice and pattern of the loading adhesive were presented. While these specific mitigation strategies were insufficient, the issue of sensor cracking is well understood with a promising path forward.

#### Acknowledgments

We gratefully acknowledge the support of the following agencies: NSERC and CFI, Canada; BMBF and HGF, Germany; and MICINN and AEI, Spain.

## References

- [1] I. Zurbano Fernandez et al., *High-Luminosity Large Hadron Collider (HL-LHC): Technical design report*, Tech. Rep. [CERN-2020-010](#), CERN, Geneva, Switzerland (2020), [DOI](#).
- [2] L. Evans and P. Bryant, *LHC Machine*, *JINST* **3** (2008) S08001.
- [3] ATLAS collaboration, *Combination of Searches for Higgs Boson Pair Production in  $pp$  Collisions at  $\sqrt{s} = 13$  TeV with the ATLAS Detector*, *Phys. Rev. Lett.* **133** (2024) 101801 [[2406.09971](#)].
- [4] CMS collaboration, *Constraints on the Higgs boson self-coupling from the combination of single and double Higgs boson production in proton-proton collisions at  $\sqrt{s} = 13$  TeV*, [2407.13554](#).
- [5] ATLAS collaboration, *The ATLAS Experiment at the CERN Large Hadron Collider*, *JINST* **3** (2008) S08003.
- [6] ATLAS collaboration, *ATLAS inner detector: Technical design report. Vol. 1*, Tech. Rep. [CERN-LHCC-97-16](#), [ATLAS-TDR-4](#), CERN, Geneva, Switzerland (1997).
- [7] ATLAS collaboration, *ATLAS inner detector: Technical design report. Vol. 2*, Tech. Rep. [CERN-LHCC-97-17](#), [ATLAS-TDR-5](#), CERN, Geneva, Switzerland (1997).
- [8] ATLAS collaboration, *Letter of Intent for the Phase-II Upgrade of the ATLAS Experiment*, Tech. Rep. [CERN-LHCC-2012-022](#), CERN, Geneva, Switzerland (2012).
- [9] ATLAS collaboration, *Technical Design Report for the ATLAS Inner Tracker Pixel Detector*, Tech. Rep. [CERN-LHCC-2017-021](#), [ATLAS-TDR-030](#), CERN, Geneva, Switzerland (2017), [DOI](#).
- [10] ATLAS collaboration, *Technical Design Report for the ATLAS Inner Tracker Strip Detector*, Tech. Rep. [CERN-LHCC-2017-005](#), [ATLAS-TDR-025](#), CERN, Geneva, Switzerland (2017).
- [11] S. Diez, *The ATLAS ITk strip local support structures*, *Nucl. Instrum. Meth. A* **1066** (2024) 169552.
- [12] Y. Unno et al., *Specifications and pre-production of  $n^+$ -in-p large-format strip sensors fabricated in 6-inch silicon wafers, ATLAS18, for the Inner Tracker of the ATLAS Detector for High-Luminosity Large Hadron Collider*, *JINST* **18** (2023) T03008.
- [13] L. Poley et al., *The ABC130 barrel module prototyping programme for the ATLAS strip tracker*, *JINST* **15** (2020) P09004 [[2009.03197](#)].
- [14] S. Kuehn et al., *Prototyping of hybrids and modules for the forward silicon strip tracking detector for the ATLAS Phase-II upgrade*, *JINST* **12** (2017) P05015.
- [15] A.L. Boebel et al., *The End-of-Substructure (EoS) card for the ATLAS Strip Tracker upgrade — from design to production*, *JINST* **19** (2024) C02067.
- [16] S. Beaupre, *Automated Assembly of Larger Detector Structures for the ATLAS New Inner Tracker*, in *13th International Hiroshima Symposium on the Development and Application of Semiconductor Tracking Detectors*, Vancouver, Canada, December 2023.
- [17] B. Stelzer, *Automated Assembly of Petals and Staves for the ATLAS New Inner Tracker Strip Detector*, in *42nd International Conference on High Energy Physics*, Prague, Czech Republic, July 2024.
- [18] CEBCA Bochnia, “MARTA (Monoblock Approach for a Refrigeration Technical Application).” <http://icp.mech.pk.edu.pl/martaco2/>.
- [19] M. Warren, “ITSDAQ Firmware.” <https://www.hep.ucl.ac.uk/~warren/upgrade/firmware>.
- [20] S. Diez Cornell, *Fighting cold noise and early breakdown on the ATLAS ITk strips tracker*, in *16th Pisa Meeting on Advanced Detectors*, La Biodola, Isola d’Elba, Italy, May 2024.

- [21] A. Tishelman-Charny, *Mitigation strategies for sensor fracturing in the ITk Strip Detector*, in *12th Large Hadron Collider Physics Conference*, Boston, USA, June 2024.
- [22] G. Vallone, H. Abidi and E. Anderssen, *Investigating Cracks in ATLAS ITk Strips*, in *12th Forum on Tracking Detector Mechanics*, West Lafayette, USA, May 2024.
- [23] Ellsworth Adhesives, “Dow SE 4445 CV Thermally Conductive Gel.” <https://www.ellsworth.com/products/by-market/consumer-products/thermally-conductive-materials/encapsulants/dow-se-4445-cv-thermally-conductive-gel-gray-210-ml-cartridge/>.
- [24] Ellsworth Adhesives, “Henkel Loctite EA 9396 AERO Epoxy Adhesive.” <https://www.ellsworth.com/products/adhesives/epoxy/henkel-loctite-hysol-ea-9396-epoxy-adhesive-1-qt-kit/>.